Research Article **ISSN: 2395 – 5597**

International Journal of Engineering and Robot Technology

Journal home page: www.ijerobot.com

https://doi.org/10.36673/IJEROBOT.2020.v08.i02.A07

PORTABLE EIGHT-CABLE ROBOT USED IN LARGE-SCALE OUTDOOR AGRICULTURE

Robert L. Williams II[*1] and Haotian Lu[1]

[1*]Department of Mechanical Engineering, Ohio University, Athens, Ohio, USA.

ABSTRACT

This research project designs a portable eight-cable robot for large-scale outdoor agriculture usage; specifically, this project designs a portable pole for the cable robot which can transport the whole system between different fields. To simplify the design, the pole will be installed onto the existing automatic moveable base, which is assuming that the pole will be installed onto the Honda's automatic ATV. Then, the system verified its stability if it can be used in the field, which means the portable poles can hold some amount of the forces with a small deflection, no tipping, and no slipping. After comparing these design parameters with other design parameters, kinematic analysis, pseudo-statics analysis, beam deflection analysis, slipping and tipping analysis, model design, and the cost estimates are done based on what is most acceptable during the project.

KEYWORDS

Cable robots, Eight-cable, Outdoor agriculture, Portable poles, Automatic moving base, Kinematic analysis, Pseudo-statics analysis, Beam deflection analysis, Slipping, Tipping analysis, Model design and Cost estimates.

Author for Correspondence:

Robert L. Williams II,

Department of Mechanical Engineering,

Ohio University, Athens, Ohio, USA.

Email: williar4@ohio.edu

INTRODUCTION

Accompanying technological development, people use robots to convenience their life, as the robot can help humans to save time or increase humans' working efficiency. For example, vacuum and mop robots are used in residents' homes for housework[1]. These robots can automatically clean their home when the residents go to work in the office, so they do not need to spend extra time on housework after a whole day's hard work. Transportation robots are used for the warehouse[2]. These robot groups are used in the storage to help workers to transport the cargos or the whole shelf to the desired location better.

Because the net system can arrange different robots to finish multiple tasks in the best order at the same time. Finally, a pertinent type of robot to this project, which is used for agriculture to grow and harvest robots[3]. These robots can help farmers finish different agriculture tasks more efficiently than humans themselves because different sensors that robots are equipped with can help the robots to make reliable choice.

Alternatively, there is another kind of robot which is the parallel robot. Compared to serial robots, cable robots have three advantages: a larger workspace, a better payload-to-weight ratio, and lower manufacturing costs[4]. Therefore, some parallel robots are already used in some fields, such as 3D printers and sky cameras[5]. They all have a similar structure that consists of an outer frame, an end-effector, and a cable system. For the 3D printer, cables move the print head around the space to print the object. For the sky camera, a camera is equipped at the end-effector so that the camera can record the sports games directly from the sky.

Additionally, some groups of researchers are focusing on using cable robots in the agriculture fields[6]. The cable robots are able to finish different agriculture tasks, but the end-effector can only work inside of the outer frame. This means that if the cable robot is used in large-scale outdoor fields for agriculture tasks, the outer frame has to be built large enough to provide enough workspace. However, the larger the frame, the higher the tension on the cable, so that the end-effector is able to maintain working ability correctly and stably when the effector works far away from the poles. For this reason, under the same winches-equipped condition, the cable robot with the larger size of the frame needs to spend more tension on maintaining the end-effector rather than the target loads. For instance, during a watering task, the weight of the water tank will be lesser than the smaller size of the frame, which means the system requires multiple cycles to finish a task. Therefore, the question of how to increase the loads while using the robots in large-scale fields becomes an issue. Then, the portable poles become a potential solution. Compared to the traditional cable robot, the poles can be transported, which means the outer frame can move in the fields freely, rather than stay fixed at a specific location. In this way, the frame can keep in a smaller size and move between the fields to finish different tasks.

In general, this research project will aim to design a portable pole for the cable robot. These portable poles should be able to hold the amount of force necessary to finish different agriculture tasks, and the portable poles should not tip or slip into the fields during work time. Therefore, the project will focus on two parts: designing a pole that can be installed onto an automatic ATV base and verifying if the poles will tip, slip, deflect, or be unable to hold the tensions to ensure that the portable poles are able to work in the field stably. Because no model will be built in the project, all of the analysis will be based on the results of the MATLAB simulations. In the simulation, some trajectories will be simulated, based on the different tracks of the end-effector in the tasks. These simulations can obtain necessary data, such as the end-effector's position, the tension on the cables, and maximum forces acting on the pole. Then, based on those data to determine will the pole achieve the design target.

Before starting the project, it is necessary to understand what fields that other projects already studied and what targets they are focusing on. Therefore, the next section will introduce some projects that use different type of robots in agriculture to complete farming tasks.

METHOD

Trajectory Description

The general structure diagram of the system is shown below to describe the motion of the end-effector while it is working in a field.

This diagram is not to scale; rather, it is meant to clarify the corresponding parts' name and origins (i.e., global origin, frame origin, and end-effector origin) and is a top view of the whole system. The four squares at the corners of the upper field, named B_i (i = 1, 2, 3, 4), are the movable poles. The area enclosed by the four poles is called field II (2), and the lower field is called field I (1). The larger square inside of field II presents as the end-effector, whose corners are referred to as P_i (i = 1, 2, 3, 4). The

cables are named from L1 to L8, as shown in Figure 1. On this diagram, there are three different origins. The global origin is set on the lower-left corner of field I, the frame origin is set on the center of pole B1, and the effector origin is set on the center of the effector. For all these different origins, x+ points right, y+ points up, and z+ points out of the paper.

Next, here are the three trajectories in this project:

Trajectory 1

The end-effector starts from the top center of the frame, then moves towards the bottom of pole 1. Next, the end-effector moves along a short straight line in the +Y direction and then stops, lifting 1m in +Z direction after the stop. After moving a short straight line in the -Y direction, shifting the end-effector back to the initial location (along the X direction). During this simulation, there are no angle changes to the end-effector.

Trajectory 2

The end-effector starts from the lower part of pole 1, 0.5meters above the earth. The end-effector then moves counterclockwise along the sides of the outer frame, from pole 1 to pole 2, then pole 3 and pole 4, and finally returning to pole 1. During the motion, the end-effector remains at the same height and includes a slight rotation in the X, Y and Z direction.

Trajectory 3

The end-effector is locked at the position closest to the lower level of pole 1, as the outer frame moves from field 1 to field 2. While the entire frame moves to the new fields, the end effector remains in the same position, with respect to the frame.

After setting up these trajectories, the MATLAB simulations are created to analyze the motions of the model, such as the simulation model for inverse pose kinematics analysis and pseudo-statics analysis. Then, the results from the simulations are used to verify if the portable poles cable robot system is usable in the field.

Inverse Pose Kinematics (IPK)

This section explains the IPK analysis. It is the most basic analysis in this project because other analyses depend on the results from the IPK. Therefore, the first step in this section is to understand what the IPK is. The IPK problem is also known as the inverse pose kinematics problem. In this kind of problem, the desired location (X, Y, Z) and the Euler angles (α, β, γ) of the end effector are established and used to calculate the required cable lengths (L_i, i = 1, 2, …, 8). Because both the location and the Euler angles of the target are considered as desired factors, the end-effector is regarded as a box rather than a point. Therefore, the center of the box is considered to be the desired location of the end-effector, and its center is presented as [0, 0, 0] in frame {P}. Because the locations of the poles are preset (P_i, i = 1, 2, 3, 4), the positions of the poles' tips and the origin point (point O = [0, 0, 0]) are also known values.

Basically, the cable length is determined by using vector operations to calculate the desired vector in a closed vector loop. In this case, the locations of most important points are known, such as the origin (point O), the top of the poles (point P_i), the location of the end effector (point T), and the top corner of the end effector (B_i). Therefore, the closed loop for finding out the cable length is the top of the poles to the box corner (P_iB_i), which is the subtract result of the original point to the box corner (OB_i) and the top poles' location to the origin point (P_iO), where $P_iB_i$is the cable length (Equation 1).

$$P_iB_i = OB_i - OP_i \quad (1)$$

If the condition for the whole system is translational moving only, then these vectors alone are needed to calculate the cable length. However, this system requires a rotation condition, which relates to the Euler angle (α, β, γ), so an orthonormal rotation matrix[7] is a necessary factor in solving this problem. The orthonormal rotation matrix [R] is listed below:

Orthonormal rotation matrix

$$[R] = \begin{bmatrix} CaCb & -SaCg + CaSbSg & +SaSg + CaSbCg \\ SaCb & +CaCg + SaSbSg & -CaSg + SaSbCg \\ -Sb & CbSg & CbCg \end{bmatrix}$$

When the system includes the rotate motion, the cable length differs from the translation-only case. The outer frame is set as the reference frame {A} in the Cartesian coordinate system and the end effector is regarded as the moving frame {P}. The frame {P} is able to move with respect to the reference frame {A}. Because the general position of the end effector is established by the desired location, and the corner

of the end effector is also known in the frame {P}, the corners' angle, in relation to frame {A}, can be represented by $[R]\{P_j\}$ (j = 1, 2, …, 4). Thus, the transformation matrix can be used to get the position of each corner in frame {A}. After the position of the effector's corner is calculated, the cable length after the effector rotated can be determined by using that result as the new OB_i.

Once the IPK problem is figured correctly, the results can be used to calculate the next section-pseudo-statics analysis. Based on this calculation, the forces acted on the portable poles can be determined, and therefore the maximum forces act on the poles are determined, which are used for the rest of the design steps.

Pseudo-statics

This section analyzes the pseudo-static equilibrium of the model, so it will examine what factors will allow for the sum of forces acting on the end-effector to be zero (free body diagram sees Figure 2). Because the velocities and accelerations of the end-effector are assumed to be small enough, the dynamic effects can be ignored during the analysis, and the whole system should be able to maintain a static equilibrium. Thus, the tensions on the cables are the main factor of the pseudo-static equilibrium to consider. These tensions can be calculated using the given values for the analysis, namely the mass of the end-effector, the external forces (or moments), and the rest of known values from the IPK. To simplify the pseudo-statics simulation in this project, the external force (or moments) that act on the effector will be assumed as zero. Then, by comparing all the tensions with the maximum designed allowable force of the portable poles, the maximum forces acting on the poles can be used to determine that they will not tip or slip from the preset location.

The vector force equation of the pseudo-static equilibrium (Equation 2.1 and 2.2) and the moment equation (Equation 3) are shown below:

$$\sum\{T_i\} + m\{g\} + \{F_{EXT}\} = 0 \quad (2.1)$$

$$\sum T_i\{unit(L_i)\} + m\{g\} + \{F_{EXT}\} = 0 \quad (2.2)$$

$$\sum M_i + [R]\{{}^{P}P_{CG}\} \times mg + r_{EXT} \times F_{EXT} = 0 \quad (3)$$

In Equation 2.1, $\{T\} = \{T_1\ T_2\ \dots\ T_8\}^T$ represents the tensions acting on the cables, $\{g\} = \{0\ 0\ -g\}^T$ is the gravity, and $\{F_{EXT}\} = \{F_xF_yF_z\}^T$ is the external forces acting on the end-effector. In Equation 2.2, unit (L_i) is the unit length of the cables. Finally, in Equation 3, $\{M_i\} = [R]\{{}^{P}P_J\}x\{T_i\}$ and $\{{}^{P}P_{CG}\}$ is $\{0\ 0\ 0\}^T$.

$$[J]\{T_i\} = -\{W_{EXT} + G\} \quad (4)$$

$$[J] = \begin{bmatrix} L1 & L2 & L3 & L4 & L5 & L6 & L7 & L8 \\ P4L1 & P1L2 & P1L3P2L4 & P2L5P3L6 & P3L7P4L8 \end{bmatrix}$$

Therefore, the Jacobian matrix (Equation 4) can be derived from Equation 2.2 and Equation 3. In Equation 4, $\{W_{EXT}\} = \{F_{EXT}\ M_{EXT} + r_{EXT}x\ F_{EXT}\}$, $\{G\} = \{mg\ [R]\{{}^{P}P_{CG}\}\}^T$. Each of the L_i in Jacobian matrix are the unit lengths of the cables and $P_j = [R]\{{}^{P}P_J\}$.

Then, Equation 4 is used to calculate the tension on the cables. However, the equation cannot be inverted directly to solve the tensions because the [J] is a 6x8 matrix (a non-square matrix). $[J]^*$ is required to solve the equation, where the $[J]^* = [J]^T([J][J]^T)^{-1}$. Therefore, the Equation 5 is derived to calculate the tensions.

$$\{T_i\} = -[J]^*\{W_{EXT} + G\} \quad (5)$$

Then, it is necessary to compare the designed allowable forces and actual forces act on the poles so that the tip and slip status of the pole can be determined. In this project, two cables are connected from a pole to the end-effector; therefore, the maximum sum of the force acted on the top of the pole can obtain from the simulation results directly. The sum of forces on X, Y, Z directions and the moments on the pole are then calculated using these simulation results and the free body diagram. If the answers are not larger than the designed values, the pole will not tip or slip (i.e., the design parameter is acceptable). Additionally, because the cable cannot push the target, all the forces need to maintain the positive tensions. Therefore, in order to avoid results that violate reality, maintaining the positive tensions in all cables is necessary. To start to address this problem, the free body diagram is presented below (Figure No.3).

Pole Deflection

In this section, because the system requests a high position accuracy, the pole's deflection is a necessary

factor to consider. In the simulation, all four poles do not bend, yet in reality, the poles will bend if the forces are large enough. For this reason, calculating the maximum deflection under maximum sum force acts on the pole is necessary. The result of unwanted deflections differs between 1 meter and 0.01 meters and can affect the end-effector's position a lot. Therefore, for this simulation, it will assume that a deflection of less than 0.05 meters is an acceptable result. In order to calculate the deflection, the singularity function of the beam deflection is used, as the diagram shows in Figure No.4.

Loading function (6)

$$q = M_A < x - 0 >^{-2} + R_A < x - 0 >^{-1} - F < x - a >^{-1}$$

Shear function (7)

$$V = M_A < x - 0 >^{-1} + R_A < x - 0 >^{0} - F < x - a >^{0}$$

Moment function (8)

$$M = -M_A < x - 0 >^{0} + R_A < x - 0 >^{1} - F < x - a >^{1}$$

Slope function (9)

$$\theta = \frac{1}{EI}\left(-M_A < x - 0 >^{1} + \frac{R_A}{2} < x - 0 >^{2} - \frac{F}{2} < x - a >^{2}\right)$$

Deflection function (10)

$$y = \frac{1}{EI}\left(-\frac{M_A}{2} < x - 0 >^{2} + \frac{R_A}{6} < x - 0 >^{3} - \frac{F}{6} < x - a >^{3}\right)$$

In these functions, M_A is the reaction moment, R_A is the reaction force, F is the load, E is the modulus of elasticity, and I is the cross-section area moment of inertia. However, there is a simplified way to calculate the beam deflection for this specific case, using the equation that is listed below:

$$\delta_{def} = \frac{F \times L^3}{3 \times E \times I} \quad (11)$$

Additionally, to avoid the pole that might yield while it is bending, a quick bending stress calculation (see Equation12) is necessary. Once the stress is lower than 36000 psi[8], i.e., 248.2 MPa, then the pole will not yield when the forces act on the pole.

$$\sigma = \frac{M \cdot c}{I} \quad (12)$$

Where M is the moment on the pole; c is the radius of the cylinder; *I* is the area moment of inertia.

Tipping and Slipping

In this section, the tipping and slipping analyses of the portable pole are separated into two 2D cases (see Figure 5). First, the force balance can be used to calculate the normal force of the pole (Equation 14). The sum of the force on the Z-direction should be equal to 0 (Equation 13), as balancing out the force is needed to find the value of the normal force. Then, the friction force is calculated based on the normal force and the friction coefficient. The maximum sum of the sub-forces that act on the top of the pole, which might cause tip or slip, are determined by analyzing the tipping (or slipping) along the X-direction (Equation 15). If the simulated results are less than the maximum sum of the sub-forces when compared to the sum of the sub-tensions along the Y-axis on the cables, then the portable pole will not tip or slip along the X-direction. A similar calculation is repeated to determine if the pole will tip or slip along the Y-direction.

$$\sum F_i = 0 \quad (i = \text{x, y, z}) \quad (13)$$

$$F_f = \mu F_N = \mu F_Z \quad (14)$$

$$\sum M_i = 0 \quad (i = \text{x, y, z}) \quad (15)$$

During the calculation, it should be noted that:

The friction coefficient is assumed as 0.36[9].

The normal forces are applied on two wheels that are on the same side equally, and the other two wheels will be regarded as having no attachment to the earth.

The sum of the sub-tensions that are applied to the cables are determined from the pseudo-statics analysis.

Control

In this section, the whole control system can be separated into two parts: 1) the movable base control and 2) the cable length control. Because the main goal of this project is not to design the whole control system, it will simply be introduced in this section.

The moving base for this project assumes the use of Honda's driverless engineering ATV[10], which should have its own complete independent control system. Because this Honda Autonomous ATV is still in the testing process, there is not much information available to the public. However, the following assumptions are made for this project: 1) the ATV can achieve the function as the movable base, 2) the

ATV can mount the designed pole successfully and 3) the ATV has 910kg to match designed parameters. The cable length control part uses the results from the IPK analysis to calculate the cable lengths, which allow the end-effector to move to the desired location. The lengths of each cable are regarded as inputs for the PID controllers. These eight independent PID controllers control the motor drivers, which apply enough current and voltage to the motors, thus controlling the cables' length and moving the end-effector to the desired position. Simultaneously, a rotary encoder (which is attached to the motor) can maintain the desired cable length changes by sending the position of the motor back to the PID controller, as the cable length can be calculated by the position of the motor and the radius of the reel.

In other words, the following factors should be present to achieve the length change control, including: A PID controller, a driver, a motor, a pulley, a sensor (encoder), and a cable. The single cable control block diagram (Figure 6) shows this below. For this whole project, eight control systems are required to cooperate with each other, using a similar structure to that of the single cable control.

System Design

Design Drawing

Results of the Example

IPK

Here are the results under Trajectory 2 conditions.

The small sharp corner on each line is caused by the step setting, as there is a short stop when the end-effector reaches the frame corners.

The whole frame moves from Field I (lower field) to Field II (upper field) with all cables locked. The four asterisk marks in Figure 12 represent the top of the poles.

As Figure No.14 shows, the end-effector starts near Pole I (B1), then runs in the counterclockwise direction to finish a rectangle. The Euler angle changes during the motion, as Figure 13 shows the alpha changes from -30 to 30 degrees, the beta changes from -20 to 20 degrees, and the gamma changes from -10 to 10 degrees.

The results of a Trajectory 1 simulation are as follows:

This simulation starts from the center of the frame at 2 meters high, then moves towards the bottom of Pole 1. Next, the end-effector moves along a short straight line in the +Y direction, stops, and then lifts 1m in +Z direction. After moving a short straight line in the -Y direction, the end-effector returns to the initial location (along the X direction). During this simulation, there are no angle changes on the end-effector.

Pseudo-statics

Some assumptions are made for the pseudo-statics analysis: 1) the end-effector's mass is 50Kg, 2) the gravity acceleration is 9.81 m/s^2, 3) the end-effector is not rotating during the motion, and 4) the analysis is based on the motion of Trajectory 1. 5) The end-effector is offset from the boundary by 1.5meters, which means the effector's actual working area (from XY face) within the 10x20 frame is 7x17 square meters. The general structure shown in Figure No.18.

According to the results from this setting, the cable tensions remain positive during the motion (see Figure No.19). This setting also maintains the static equilibrium rules while simulating. Additionally, the singularity-check also maintained results above 0 (see Figure No.20).

In order to obtain the correct maximum forces acting on the pole, these forces should be the largest sum force act on the pole in the simulation. Therefore, in the specific trajectory 1 simulation, the largest sum force is found at the beginning of the motion, which is located in the center upper region of the field; In addition, according to the cables' setting, design candidate 5^{11}, the sum forces acting on each pole are also necessary to be calculated and compared to get the real maximum one. According to Figure No.21, the result clearly showed that the maximum sum force is acting on pole 1, therefore the tipping and slipping analysis will be based on pole 1 and the result is shown below:

It should be noted that the results from this simulation are very sensitive to the boundary parameters, especially to the end-effector's offsets to the boundary of the field. When the end-effector moves too close to the boundary, some negative tension occurs in the tensions feedback. Negative

tension feedback also occurs in the simulation when the motion is limited to a small space in the upper center region. Therefore, to avoid the negative tensions occurs on the cables, the boundary parameters is an important factor to be considered.

Pole Deflection

The material of the pole should be considered. Because it will be used in outdoor fields, environmental corrosion is an issue. Additionally, it should be able to hold some force without unwanted deflection, as those unwanted deflections will affect the position accuracy of the end-effector. Therefore, a solid steel round bar (A36) is used for this design. Given a steel pole and based on the singularity function of the beam deflection, the related values can be calculated and listed below:

As seen in Table No.2 and Table No.3, when the pole's diameter is 0.0762 m, the maximum sum force acts on the top of the pole, causing a 0.02m deflection, which should be acceptable. Additionally, to avoid the pole that might yield while it is bending, a quick bending stress calculation is shown below. The bending stress is much lower than the yield point, therefore the pole should be safe.

$$\sigma = \frac{M \cdot c}{I}$$

$$\sigma = \frac{6015.13 \times 0.0381}{1.655 \times 10^6} = 1.389 \times 10^8\ Pa$$

$$= 138.9\ MPa$$

$$\sigma < \sigma_{yield}\ (248.2\ MPa)$$

One thing that needs to be noticed, it is possible to use a hollowed pole in the system to reduce the weight of the bar, and convenience workers to install or replace it. However, it needs to make sure to correct the calculations to ensure the system can work correctly.

Tipping and Slipping

The analysis of the tipping and slipping of the pole is based on Table No.2 and Table No.3. However, there are some additional factors that need to be assumed:

Based on the information from Huntley[12].

The ATV is assumed as 2 meters × 2 meters × 1 meter.

The mass of the ATV is 910 Kg. Currently, the heaviest human-driven one is around 427Kg, but the model requires a heavier ATV to maintain the balance.

The friction of the earth is 0.36[9].

All of the forces are regarded as the point loads.

Counterclockwise is the positive direction.

Pole 1 is the example for this analysis, and its mass is 64.03kg.

The maximum tensions applied from the cables are obtained from the MATLAB simulation and listed below.

Y-Z face

$$\sum F_Z = -mg_{bar} - mg_{ATV} + F_N = 0$$

$$F_N = 9545.91\ N$$

$$F_{12Y} = F_{1Y} + F_{2Y} = 2988.95\ N$$

$$\sum F_Y = F_Y - \mu F_N = 0$$

$$F_Y = 0.36 \times 9545.91 = 3436.5\ N > F_{12Y}$$

$$\sum M_X = mg_{bar} \times 1.5 + mg_{ATV} \times 1 - F_Y \times 2.8 = 0$$

$$F_Y = 3524.7\ N > F_{12Y}$$

Based on the sum moment equation (from the Y-Z case), the critical tipping tensions are larger than the cables applied, so the pole is not tip into the field; Also, the critical slipping tensions are larger than the cables applied, so the pole is not slipping into the field.

X-Z face

$$\sum F_Z = -mg_{bar} - mg_{ATV} + F_N = 0$$

$$F_N = 9545.91\ N$$

$$F_{12X} = F_{1X} + F_{2X} = 1494.46\ N$$

$$\sum F_X = F_X - \mu F_N = 0$$

$$F_X = 0.36 \times 9545.91 = 3436.5\ N > F_{12X}$$

$$\sum M_Y = -mg_{bar} \times 1.5 - mg_{ATV} \times 1 + F_X \times 2.8 = 0$$

$$F_X = 3524.7\ N > F_{12X}$$

In this case, the critical tensions are larger than the cables applied, so the pole will not tip or slip into the field.

$$\sum F_{XY} = \sqrt{F_{12X}^2 + F_{12Y}^2} = 3341\ N$$

$$F_f = \mu F_N = 0.36 \times 9545.91 = 3436.5\ N > F_{XY}$$

After comparing the sum of the horizontal sub-forces with the maximum static friction, it can be concluded that the pole will not slip while the system is working. However, since the maximum horizontal sum forces and the maximum static friction between the tire and the field are close, it is necessary to pay attention to the external forces that may act on the effector. If there are external forces such as wind or rains, the poles may start to tip or slip.

Cable Length Control

Figure No.24 shows the general block diagram for controlling the eight cables with PID controllers. The input of the system is the desired pose of the end-effector, which is its cartesian coordinate (X, Y, Z) in the working field, and its Euler angles (α, β, γ) with respect to the global origin. Then, the IPK analysis is used to calculate each cable's length from the poles to the target location, and those lengths can be inputted into the corresponding cable's PID controller. As Figure No.24 shows, these eight cables are controlled parallelly and they all have same structure (a PID controller, a driver, a motor, a pulley, an encoder, and a cable), but different input values.

Therefore, using one line as the example, once the PID controller receives the length input, it will apply the proper amount of current and voltage to drive the motor to the correct rotation speed. Then the motor can control the cable by releasing or rolling in to change the cable length and change the direction of the cable via the pulley. Additionally, an encoder attached on the motor can send the feedback to the controller to adjust the motor's status (speed up, stay, speed down, or stop). By combining the eight cables' length change, the end-effector can reach the target position with the desired angle. Additionally, there is another possible solution to set the control system that can also achieve to control the 8 cables, which is to use a multi-axis PID controller to control all eight cables (see Figure No.26).

Orthonormal rotation matrix

Sa=sin(α)	Sb=sin(β)	Sg=sin(γ)
Ca=cos(α)	Cb=cos(β)	Cg=cos(γ)

Table No.1: General parameters for system setting

S.No	Factor	Value	Unit
1	End-effector size	0.5	m
2	Poles height	2.8	m
3	Field size (L)	20	m
4	Field size (W)	10	m

Table No.2: General values of the pole

S.No	A36 Steel					
1	L	1.8	m	volume	0.00821	m^3
2	r	0.0381	m	density	7800	kg/m^3
3	D	0.0762	m	mass	64.03	kg
4	d	0	m	weight	628.11	N
5	Ix	1.65E-06	m^4	1/EI	3.02E-06	
6	E	200	Gpa	2E+11	Pa	
	Deflection				0.020	m

Table No.3: Forces on the Pole

S.No		1	2	F12_sum			
1	F	850.90	2500.35				
2	X	-402.36	-1092.10	X	-1494.46	F_{xy}	3341.74
3	Y	-747.25	-2241.70	Y	-2988.95	M	6015.13
4	Z	61.31	183.94	Z	245.25		

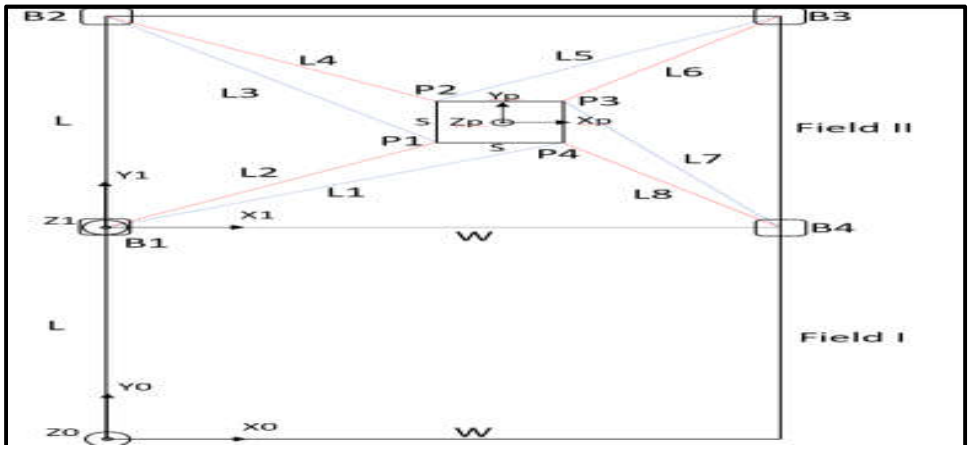

Figure No.1: General diagram of the system

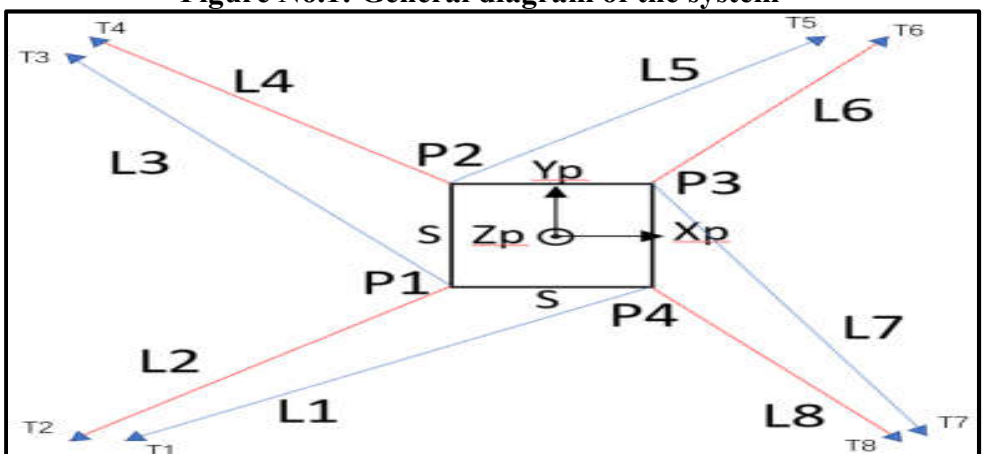

Figure No.2: Pseudo-static free body diagram

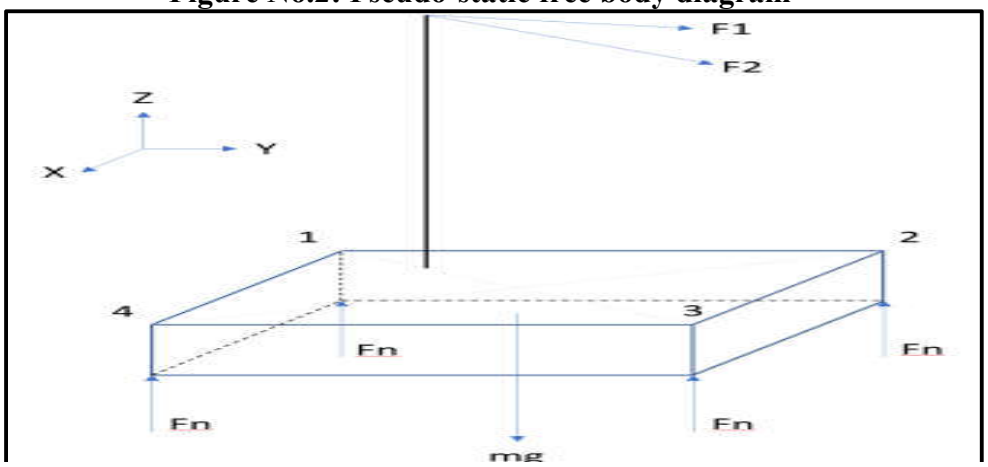

Figure No.3: Free body diagram of the pole

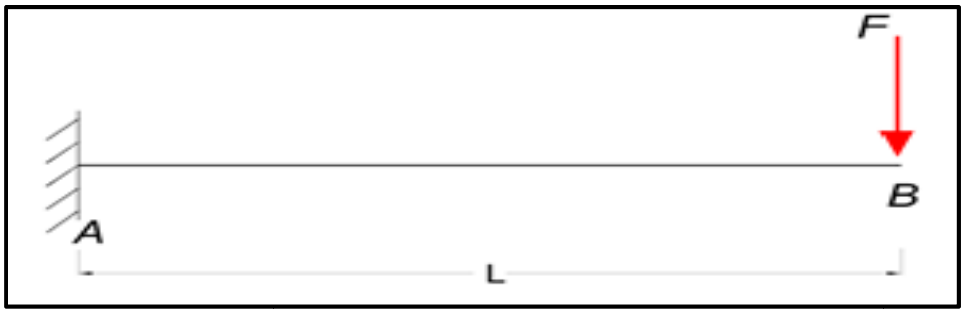

Figure No.4: Single load at the end (Engineering Tool Box, n.d.)

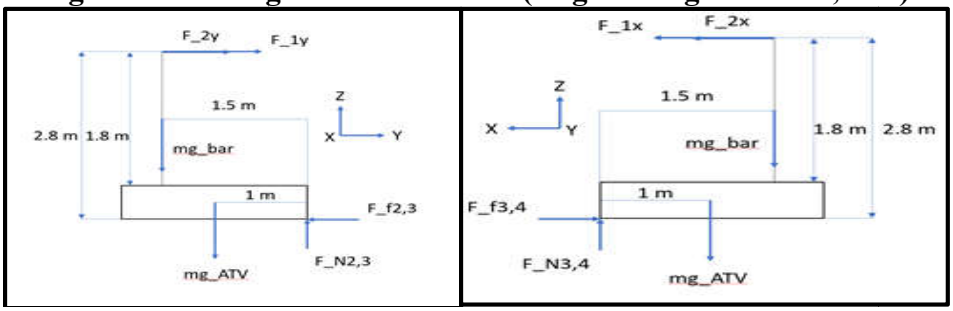

Figure No.5: Free body diagram in 2D cases (FBD)

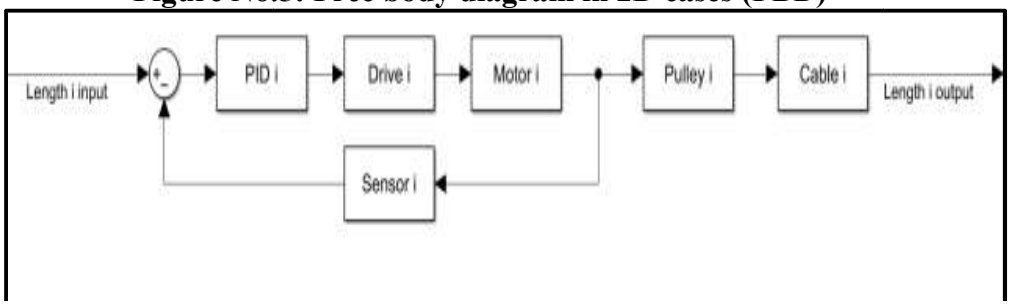

Figure No.6: Block Diagram for single cable control with a PID controller

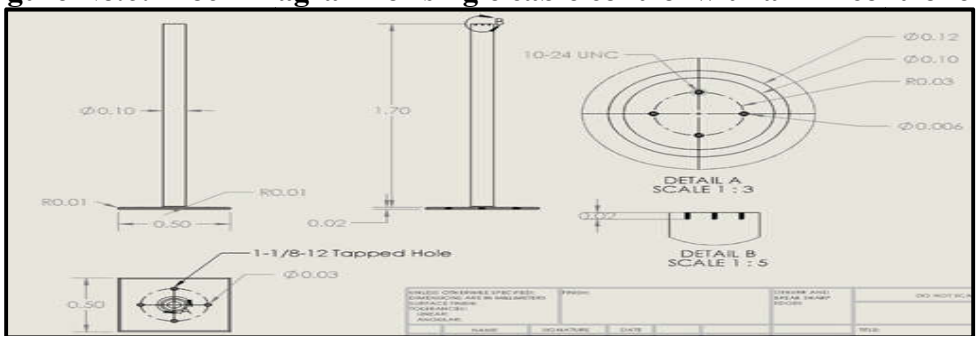

Figure No.7: Drawing for the pole

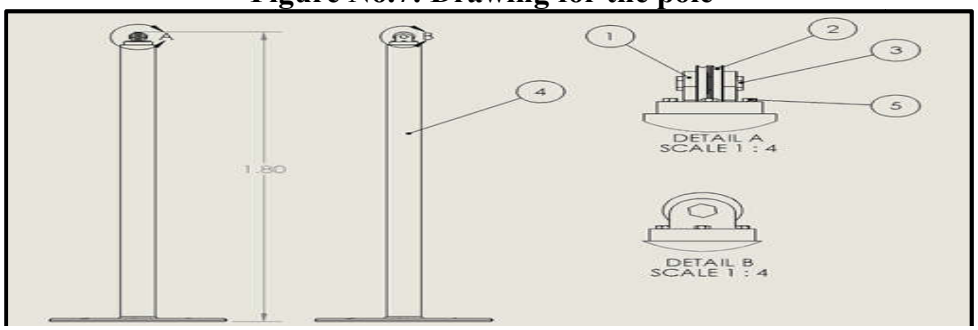

Figure No.8: Drawing for the Pole with the Pulley

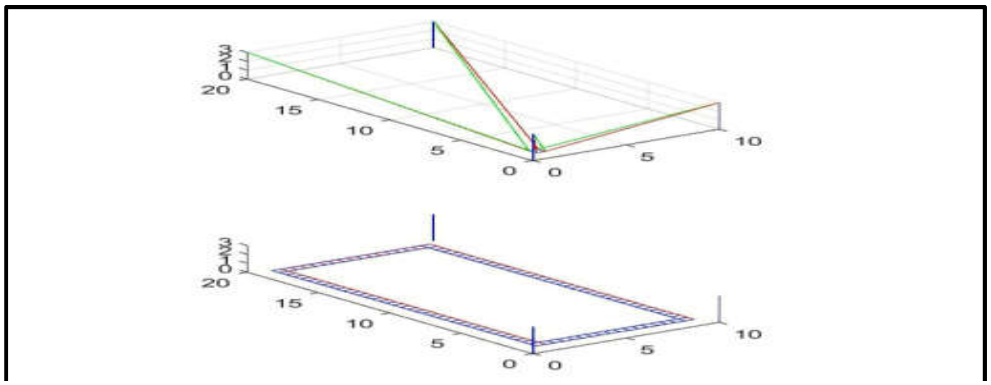

Figure No.9: Structure of the frame for the end-effector's rectangular motion

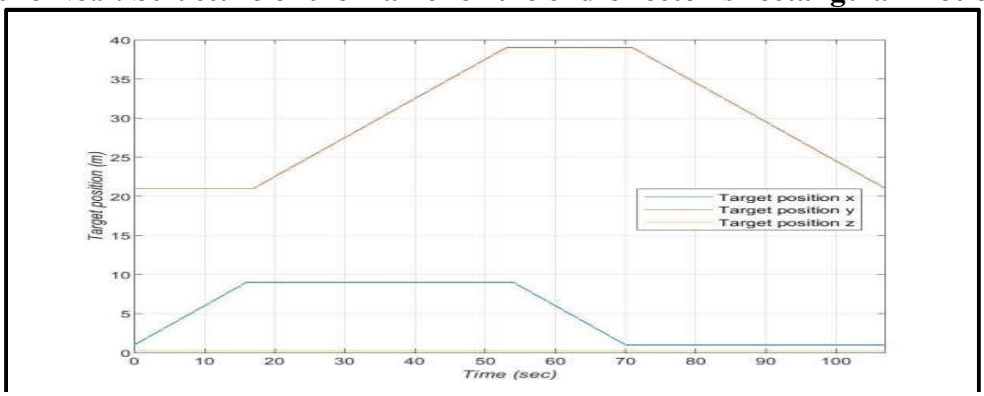

Figure No.10: Position of the end-effector changes during the rectangular motion

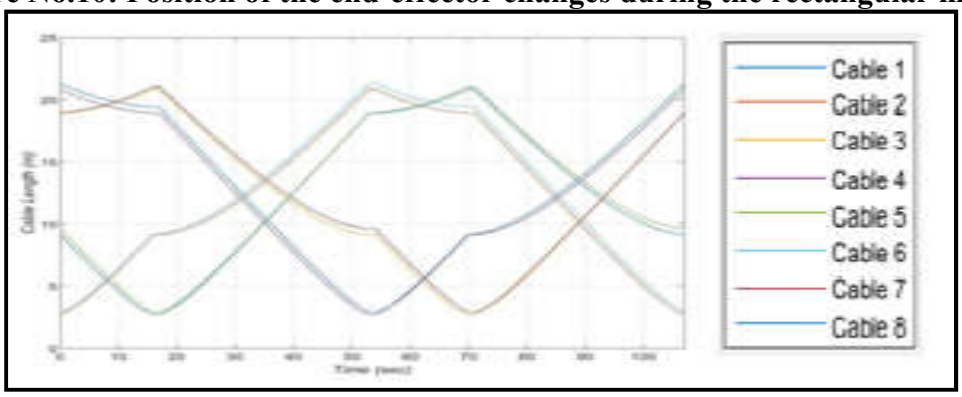

Figure No.11: The cable length changes while in motion

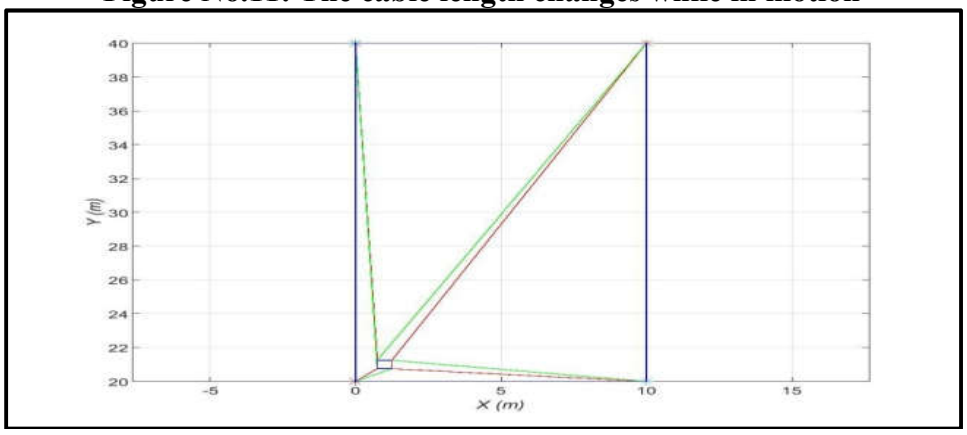

Figure No.12: Frame moves from Field I to Field II with all cables locked

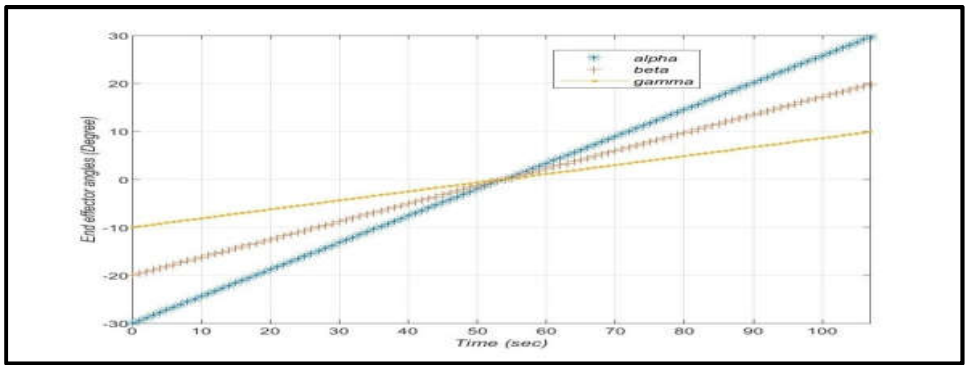

Figure No.13: The end-effector's angle changes while in motion

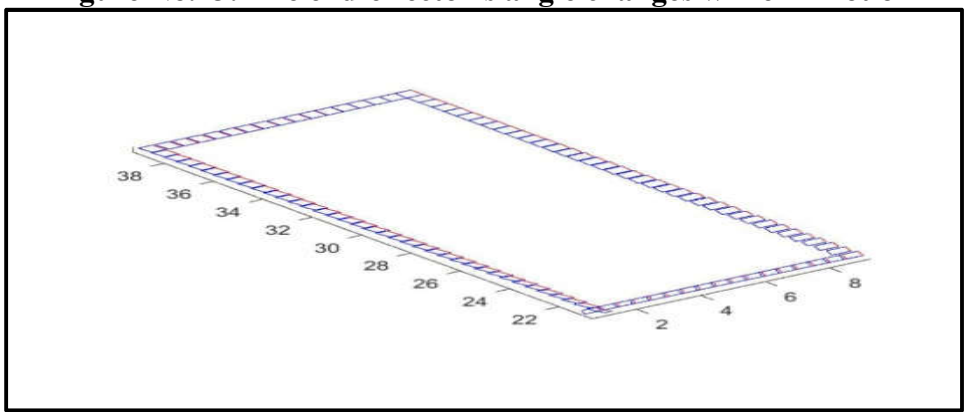

Figure No.14: The track of the end-effector's motion

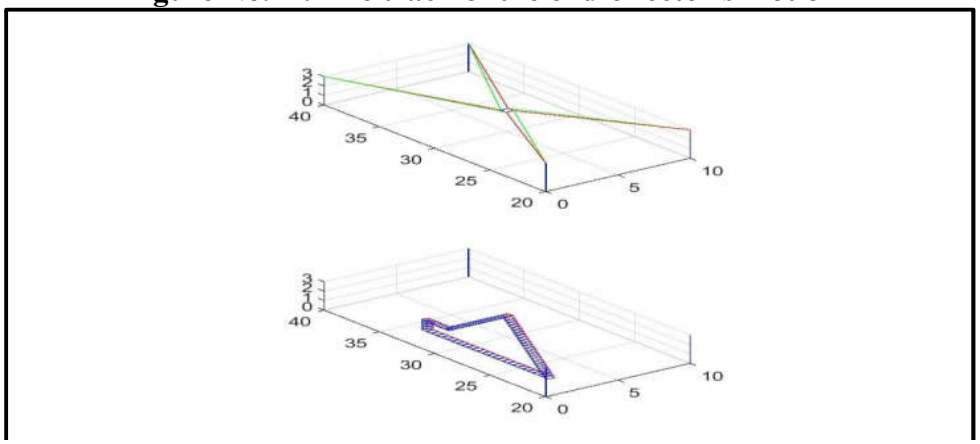

Figure No.15: General motion track

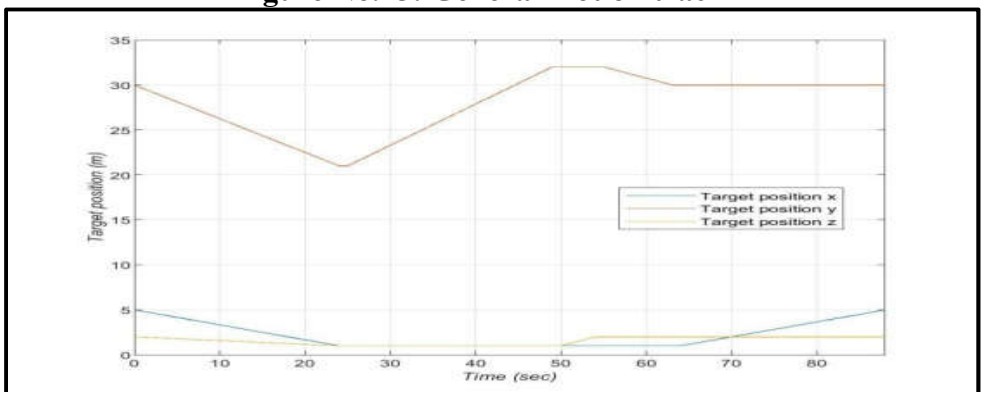

Figure No.16: Position of the end-effector changes in Trajectory 1

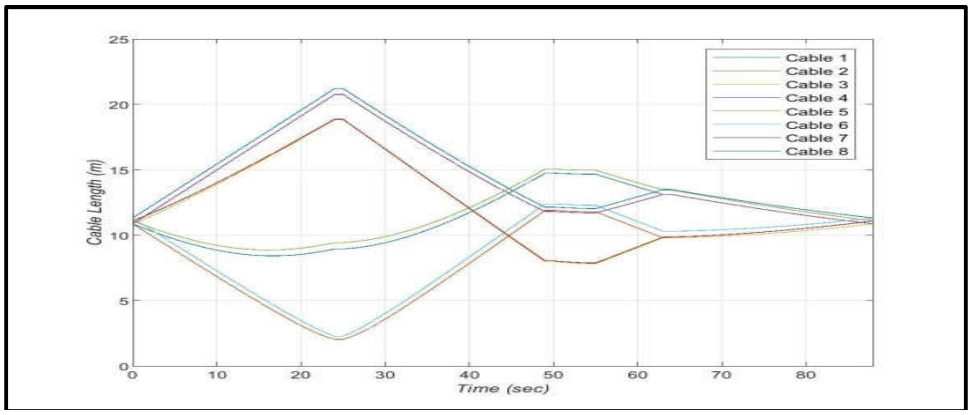

Figure No.17: The cable length changes while motion

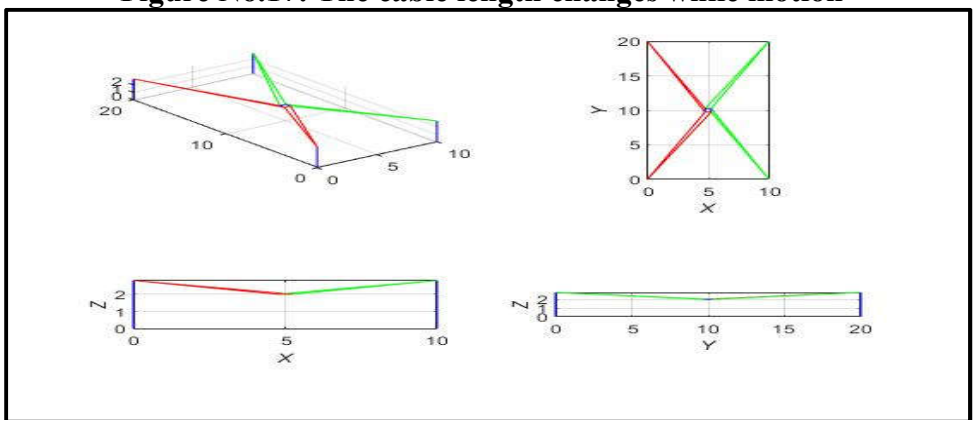

Figure No.18: Structure of the system and the three side views

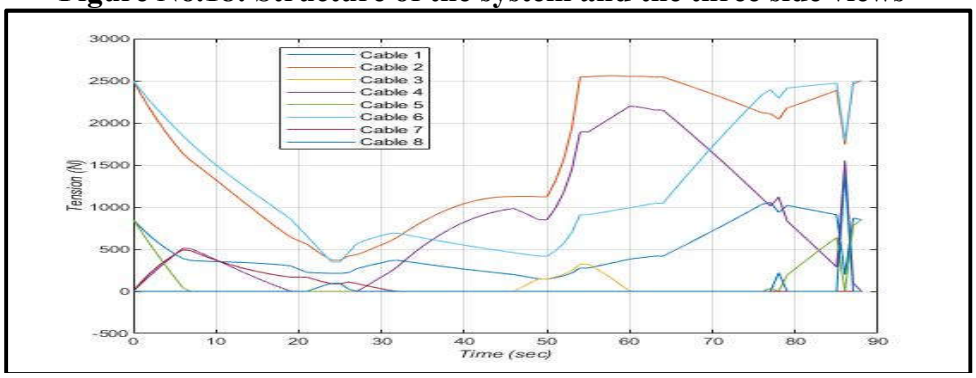

Figure No.19: Cable tensions vs. time

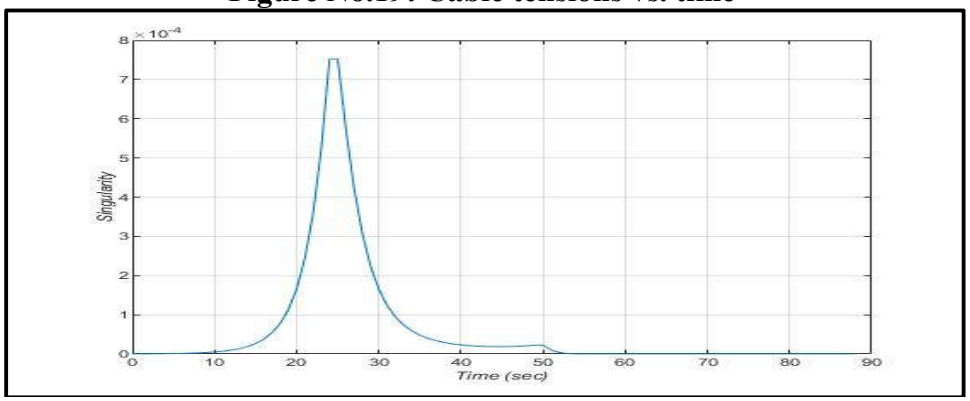

Figure No.20: Singularity vs. time

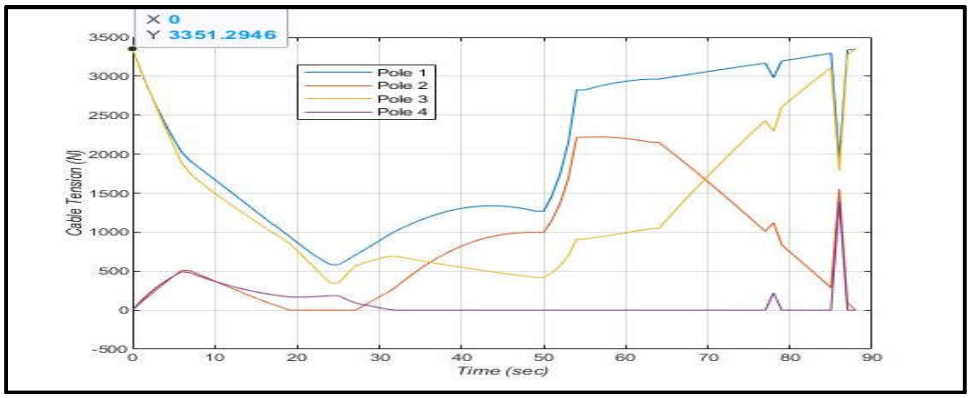

Figure No.21: Sum of forces acting on each pole over time

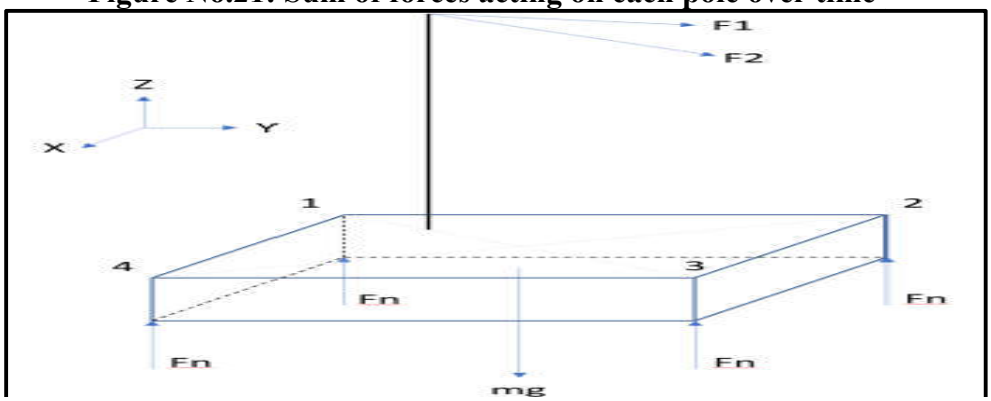

Figure No.22: Free body diagram (FBD)

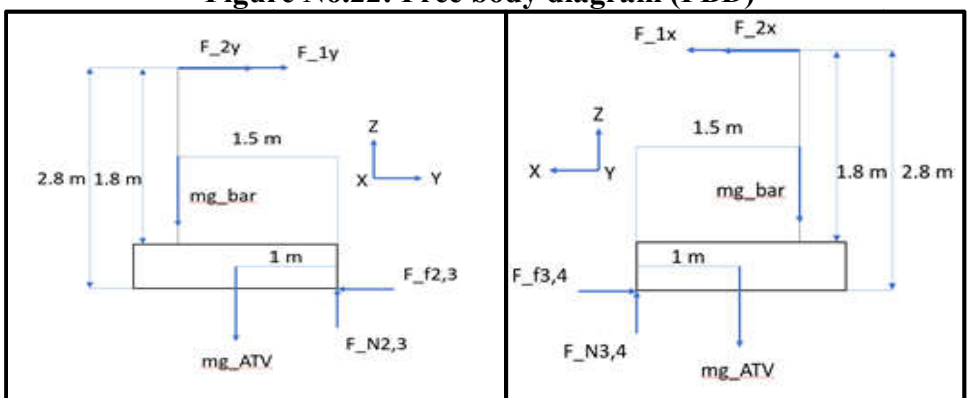

Figure No.23: Free body diagram in 2D cases (FBD)

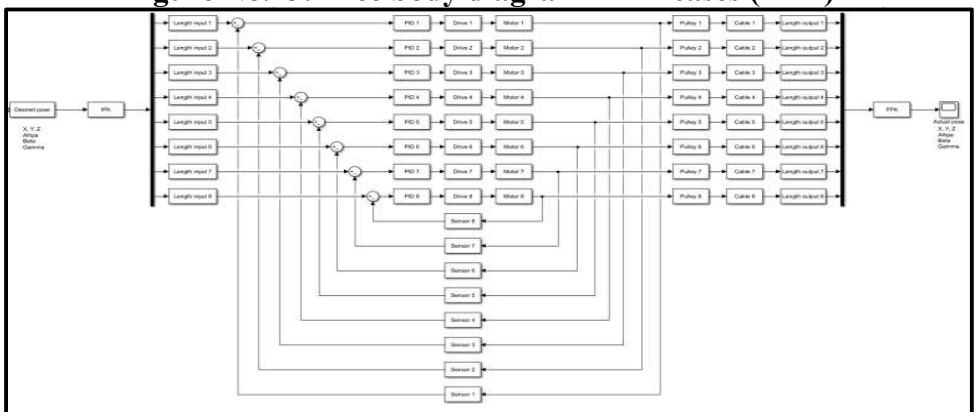

Figure No.24: General block diagram for eight cables control with PID controllers

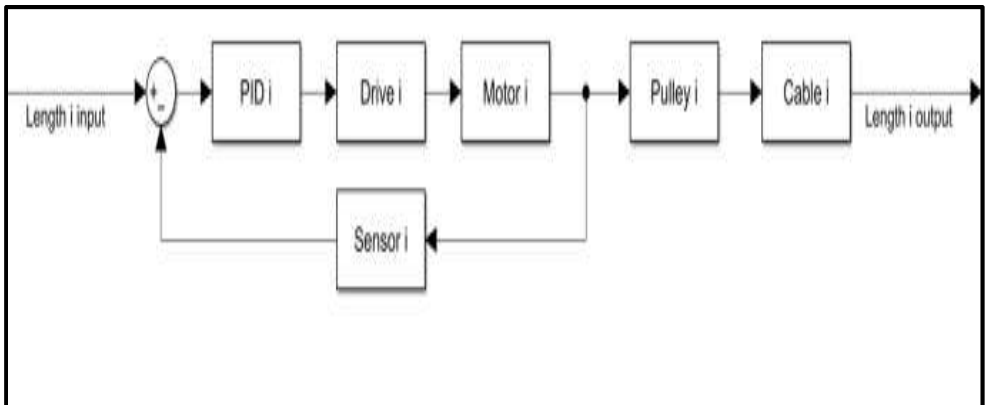

Figure No.25: Block diagram for single cable control with a PID controller

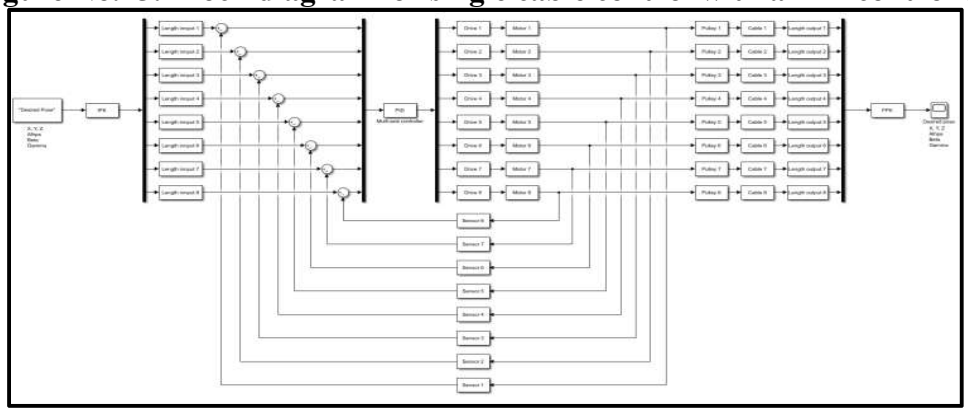

Figure No.26: Block diagram for eight cables control with multi-axis PID controllers

CONCLUSION AND FUTURE WORK

Conclusion

This paper proposes that the eight-cables robot, which uses the structure of Design Candidate 5, can be used in the agriculture field based on MATLAB simulation. In the simulation, the corners of the square end-effector platform are connected to the tops of four portable poles by eight cables. Controlling the length of these eight cables can move the effector to the desired location with a specific pose (row, pitch, and yaw), and during the simulation, this effector can accomplish some trajectories, which are regarded as the motion's track for the agriculture tasks. After completing kinematics analysis, pseudo-static analysis, pole deflection, and tipping and slipping analysis and considering the positive tensions on the cables and singularities, all the results proved that this eight-cables robot can theoretically be used in the field to accomplish agriculture tasks. Additionally, the kinematics analysis indicated that the entire frame can be moved from field to field with all cables locked.

While the design works in a simulation the many assumed pre-set values can cause the results to differ from reality. For example, assuming that no rain and wind loads act onto the end-effector ignores real environmental conditions, the straight cable used in the project was assumed to be ideal and massless, but in the real world, it has mass. Finally, the earth friction coefficient was assumed to be 0.36, when in reality, it varies based on different surfaces. All of these will impact the reality performance of the cable robot. These assumed values, even under the logical assumption, are still potential uncertain factors that can affect real-world results because there is no model that can collect real data that would correct for the errors from the assumptions. In addition, the main part of the portable pole is the movable base, but that driverless engineering ATV is still in test progress, which means there is little information about it. It becomes another uncertain factor in the project.

The Unique Contribution of the Research Work

Some groups have used serial robots in the agriculture field to take care of plants, and a small group of factories have mentioned using cable robots. However, those that do use cable robots utilize fixed poles in the fields rather than portable poles. Because portable poles can be transported between different fields and the size of the frame can be adjusted to be made more accessible, the portable poles cable robot can be used to explore agriculture.

ACKNOWLEDGEMENT

The authors wish to express their sincere gratitude to Department of Mechanical Engineering, Ohio University, Athens, Ohio, USA for providing necessary facilities to carry out this research work.

CONFLICT OF INTEREST

We declare that we have no conflict of interest.

BIBLIOGRAPHY

1. Johnson D. Get the Neabot self-emptying robot vacuum for $365, an all-time low price, *CNET,* 2021.
2. Dawson C. Alibaba has the largest AGV 'Robot' army in China, Tamebay, *Channel IX,* 2018.
3. Brigham K. This start-up created the first farm in America run entirely by robots, *CNBC,* 2018.
4. Qian S, Zi B, Shang W W, Xu, Q S. A Review on cable-driven parallel robots, *Chinese Journal of Mechanical Engineering,* 31(1), 2018, 1-11.
5. Stadium-sized 3D printers using winch robots (aka Cable Robots or Rope Robots), 2014.
6. Radojicic J, Surdilovic D, Kruger J. Application challenges of large-scale wire robots in agricultural plants, *IFAC Proceedings Volumes,* 46(4), 2013, 77–82.
7. Craig J J. Introduction to robotics: Mechanics and control, *Addison Wesley Publishing Co., Reading, MA,* 2005.
8. Metals Depot. A36 steel round bar. *Metals Depot*.
9. Engineering tool box. Friction and friction coefficients, *Engineering Tool Box*.
10. Cheng M. Honda unveils an autonomous ATV for industrial and agricultural use, *Future Car,* 2018.
11. Williams II, R L, Graf E. Eight-cable robocrane extension for NASA JSC ARGOS, *Volume 10: 44th Mechanisms and Robotics Conference (MR)*, 2020.
12. Huntley B. How big is an ATV? A guide to ATV dimensions by engine size, *ATV Man,* 2018.

Please cite this article in press as: Robert L. Williams II and Haotian Lu. Portable eight-cable robot used in large-scale outdoor agriculture, *International Journal of Engineering and Robot Technology,* 8(1), 2021, 42-57.